OPTIMAL PID CONTROLLER BASED AUTOPILOT DESIGN AND SYSTEM MODELLING FOR SMALL UNMANNED AERIAL VEHICLE

Róbert SZABOLCSI

Óbuda University, Budapest, Hungary (szabolcsi.robert@bgk.uni-obuda.hu)

DOI: 10.19062/1842-9238.2018.16.3.6

Abstract: *The Proportional-Integral-Derivative (PID) controller is often considered for an old fashion technique. However, from the early 1910's it has been deeply penetrated in many control applications. The impressive history of PID controllers and experiences gained from their wide-broad control applications assign to emphasize that it is still a promising solution in a given set of control applications. Most of the commercial autopilots available for use unmanned aerial vehicle (UAV) aboard must be hand-tuned when it is installed in the UAV. This requires a well-trained, experienced UAV operator, or, ground maintenance staff able to set the PID controller parameters proper to given UAV flight mission and proper for the flight conditions during the entire flight time. The early commercial-off-the-shelves (COTS) UAV autopilots used the PID controller to steer the UAV. Recently, the PID controller is not forgotten, and, there is an intensive spread and deep penetration of the PID controllers applied for UAV automatic flight control. The purpose of the author is to highlight the control problem of the PID controller tuning, and, to introduce a new enhanced PI controller. The MATLAB scripts are created by the author supporting controller parameters' tuning activity of the UAV operators, or of the ground maintenance staff to minimize time required, and to maximize readiness of the UAV for flights.*

Keywords: *UAV, UAV automatic flight control, PID-Controller, MATLAB.*

1. INTRODUCTION

Unmanned aerial vehicles (UAV) are widely spread ones both in military and civil applications. Some UAVs famous for its robust automatic flight control systems ensuring appropriate level of the flight safety comparable to that of the manned aircraft. Regarding several national regulations, there is a general rule that not necessary to apply autopilot on the board. However, if to implement it, the onboard autopilot can support UAV operators in execution of the flight missions, regulating appropriate flight parameters, ensuring automation of the safe return to home, and, in case of necessity, the automated emergency landing is also can be executed autonomous way.

There are many sellers trading with universal autopilots, like MP2028g2, MP2128g2, or, Paparazzi. The universal feature of the autopilots is an advantage, i.e. they can be implemented on the board of the wide range of the different UAV types. The universality means and requires high level of skills whilst to schedule and fit it to the given UAV platform. This study proposes an analytic method of gain scheduling of the autopilots, as the first steps in setting and defining PID-controllers' parameters.

Thus, importance of the heuristic gain selection is reduced and replaced by the analytic one of the pole placement technique. This analytic controller design method and, computer simulation can support UAV users in gain fitting and scheduling.

2. LITERATURE REVIEW

In spite of being relatively old fashion ones, PID-controllers still widely used both in classical and modern control engineering. Past decades modern robot applications like ground and air robots due to its privileges the PID-controller based platforms gained special attention, which are thoroughly examined in [4, 5, 6, 7, 8, 9, 11, 12, 15, 16, 17]. The affordability, the price and, finally, experiences captured in several applications of modern robotics, allowed to keep this technique at top level, and development of PID-controllers still is ongoing [21, 22].

Moreover, solution of many controller design and scheduling problems are traced back to PID-controllers, and powerful computer software support is available [19, 20].

The evolution of the UAVs is deeply analyzed in [14], and its military application in integrated air defense systems is examined in [10].

In [1] there is a competing controller synthesis design method of the famous linear quadratic regulation problem (LQR) is used to design stabilizing controller for the UAV. In the article of [18] selection of the different weighting matrices needed to solve the LQR design problem is thoroughly examined and solved, based on aerodynamic data of the small fixed-wing UAV [2, 13]. Problems related to the solution of the redundancy problems aboard of the UAV are exhaustively investigated in article of [3].

3. FUNDAMENTALS OF THE PID-CONTROLLER

The traditional PID-controller consists of three branches connected parallel way to each other. The series feed-forward representation of the PID-controller can be seen in FIG.1.

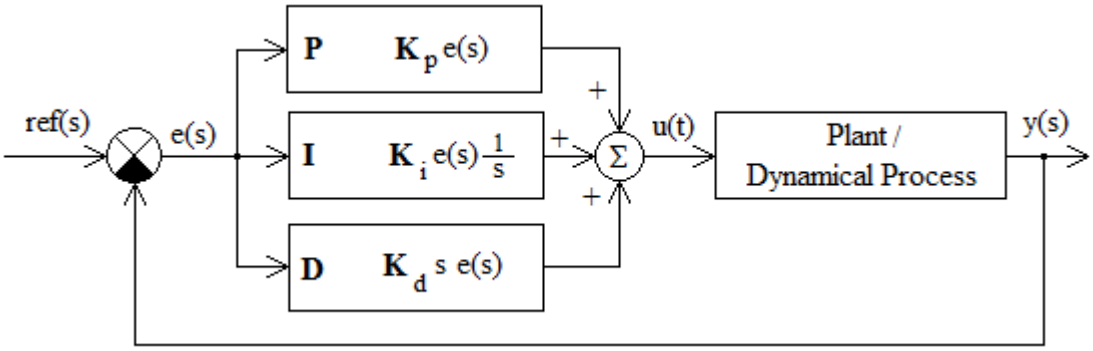

FIG. 1 Closed Loop System Block Diagram with PID Controller in Feedforward Path.

The closed loop system mission is to establish at system output the measured output of *y(t)*, which is itself represents response to that of the desired process value of *ref(t)*. The controller mission is to minimize, or as the best case, nullify the error of *e(t)* over time of *t* by adjusting control variable of *u(t)*, such as to deflect aerodynamic control surface of the aircraft to its new position determined by a weighted sum of the three control terms in the PID controller.

The term P(proportional) in the PID controller is the proportional to that value of the error e(t). The ideal I(integral) term accounts for the past values of the error *e(t)*, and integrates it over time. Finally, the ideal D(derivative) term represents the best estimate of the future trend of the error signal *e(t)*, and it is generated by the rate of error change of $\dot{e}(t)$. The more rapid changes are in error e(t), the greater is the closed loop damping via increasing amount of energy existing in total sum of the control efforts of the basic terms in the controller.

The balance between those three control terms depends on those dynamic performances and requirements set for the closed loop control system. That tuning requires a priori knowledge of external disturbances and sensor noises shifting process variable *y(t)* apart from its desired one.

Thus, in many control applications, the lag-, the lead-, or the lead-lag compensator is used to eliminate bottlenecks of the application of the idealized I-, or D-terms.

3. PID-CONTROLLER OPTIMAL DESIGN USING OPTIMAL LINEAR QUADRATIC APPROACH

To highlight design problem being solved the small UAV will be considered. The aerodynamic model of the lateral motion of the small fixed-winged UAV Boomerang-60 Trainer UAV is as follows [2, 18]:

$$\dot{\boldsymbol{x}} = \boldsymbol{Ax} + \boldsymbol{Bu} = \begin{bmatrix} \dot{v} \\ \dot{p} \\ \dot{r} \\ \dot{\phi} \end{bmatrix} = \begin{bmatrix} -0{,}7724 & 0 & -18{,}9671 & 9{,}0867 \\ 1{,}9247 & -19{,}9149 & 7{,}7565 & 0 \\ 69{,}1314 & -23{,}8689 & -2{,}5966 & 0 \\ 0 & 1 & 0 & 0 \end{bmatrix} \begin{bmatrix} v \\ p \\ r \\ \phi \end{bmatrix} + \begin{bmatrix} 0 & 2{,}2582 \\ -23{,}8289 & 1{,}5015 \\ -11{,}7532 & -15{,}2855 \\ 0 & 0 \end{bmatrix} \begin{bmatrix} \delta_a \\ \delta_r \end{bmatrix} \quad (1)$$

In equation 1 v is the lateral speed, p is the roll rate, r is the yaw rate, ϕ is the roll angle position, δ_a is the angular deflection of the ailerons, and, finally, δ_r is the change in rudder angular position. In [18] the reduced short period motion dynamic model is used to be:

$$\dot{\boldsymbol{x}} = \boldsymbol{Ax} + \boldsymbol{Bu} = \begin{bmatrix} \dot{p} \\ \dot{\phi} \end{bmatrix} = \begin{bmatrix} -19{,}9149 & 0 \\ 1 & 0 \end{bmatrix} \begin{bmatrix} p \\ \phi \end{bmatrix} + \begin{bmatrix} -23{,}8289 \\ 0 \end{bmatrix} \delta_a \quad (2)$$

Using matrices **A** and **B**, and supposing a two dimensional identity matrix for **C**, and zero matrix for feed-forward matrix **D** in the state space model, the system was controllable and observation has been examined. The short period (single degree-of-freedom) motion dynamic model is we have dealt with is controllable and observable.

The block diagram of the UAV autopilot proposed can be seen in FIG. 2.

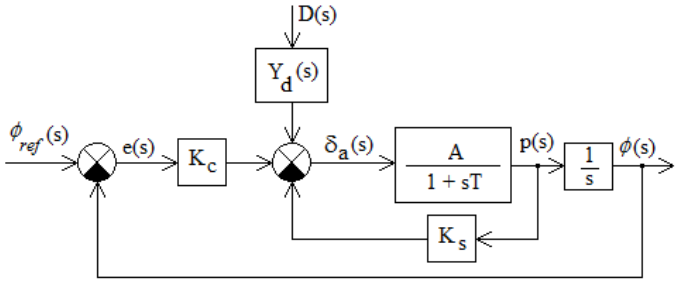

FIG. 2 Roll Angle Autopilot of the UAV with External Disturbance.

The feedforward controller is represented with P-term as the first trial to be used for design of the optimal LQR controller. In [18] the design problem is solved for following weights applied in LQR problem solution:

$$\boldsymbol{Q} = \begin{bmatrix} 1 & 1 \\ 0 & 10 \end{bmatrix};\ \boldsymbol{R} = 1 \tag{3}$$

The optimal full state feedback gain matrix $\boldsymbol{K}$ and the cost matrix $\boldsymbol{P}$ are calculated to be [18]:

$$\boldsymbol{K} = [K_s \quad K_c] = [0.5656 \quad 3.1623];\ \boldsymbol{P} = \begin{bmatrix} 0.0237 & 0.1327 \\ 0.1327 & 4.4316 \end{bmatrix} \tag{4}$$

Using Eq. 1 gain and time constant of the UAV dynamics can be derived to be:

$$A = 1{,}196536262;\ T = 0{,}050213659\ s \tag{5}$$

The time domain analysis of the autopilot of the UAV represented in FIG.3 [19, 20].

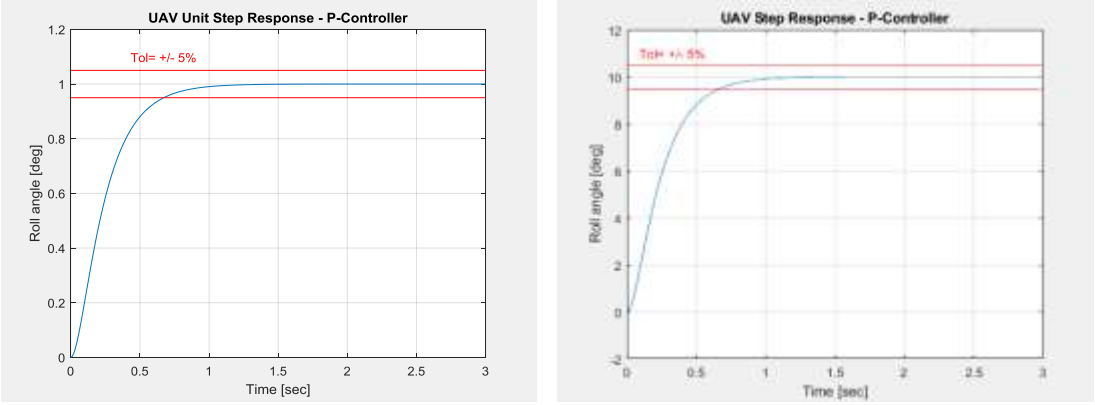

(a) $\phi_{ref}(t) = 1 * 1(t)\ deg$ (b) $\phi_{ref}(t) = 10 * 1(t)\ deg$

FIG. 3 Time Domain Analysis of the UAV Closed Loop Automatic Flight Control System. (MATLAB-script: R. Szabolcsi).

From FIG. 3 it is evident that if to set 5% of tolerance field to derive settling time, for the case when the UAV autopilot is subjected to unit change in roll angle, the settling time is ≈ 0,6 sec, whilst for more intensive maneuvers, when the desired value of the roll angle at the closed loop control system input is 10 deg., the settling time is increased till that of ≈ 0,7 sec. In spite of being increased, the settling time is still kept in the range of proper and acceptable time range ensuring agile response of the UAV to the control reference input of the roll angle being stabilized.

Stability of the roll angle autopilot closed loop control system can be evaluated using FIG. 4 [19, 20]. From FIG. 4 it is evident that calculated closed loop poles are negative ones, i.e. they lie on the left-hand side of the complex plain. This means, that closed loop system time domain behavior is stable, being aperiodic, exponential one, and settling time t_{ss} mostly determined by the pole being real located at *(-5,08+0*j)*.

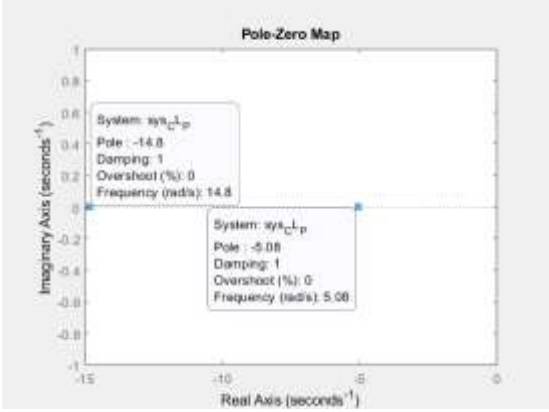

FIG. 4 Pole-Zero Map of the UAV Closed Loop Automatic Flight Control System – P-Controller Case (MATLAB-script: R. Szabolcsi).

The closed loop control system stability is also can be examined using open loop system Bode diagrams [19, 20]. The roll angle autopilot open loop control system Bode diagram, with stability margins can be seen in FIG.5.

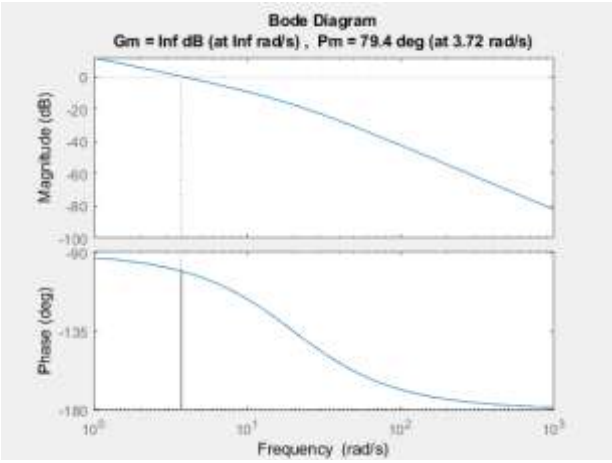

FIG. 5 UAV Open Loop System Bode Diagram – P-Controller Case (MATLAB-script: R. Szabolcsi).

From FIG. 5 it is easily can be determined that the closed loop automatic flight control system of the UAV is stable one due to infinite gain margin and due to positive phase margin of +79,4 degrees measured at 3,72 rad/sec crossover frequency. It is evident, that in case of positive gain and phase margins the UAV roll angle closed loop control system is stable.

The UAV autopilot closed loop control system based upon P-controller has been tested for disturbance rejection ability. The external disturbance considered to behave with unit step feature, i.e. *D(t)=1*1(t)*, and, there is no change in roll angle reference, i.e. $\phi_{ref}(t) = 0$. Results of the computer simulation can be seen in FIG. 6 [19, 20].

Using final value theorem of the well-known Laplace-transformation yields to:

$$\lim_{t\to\infty} \phi(t) = \lim_{s\to 0} s\phi(s) = \lim_{s\to 0} sW_D\,(\mathrm{s})\mathrm{D}(\mathrm{s}) = \lim_{s\to 0} W_D\,(\mathrm{s}) = \frac{1{,}1965}{0{,}002521s^2+1{,}6767s+3{,}7821} \cong 0{,}3162 \text{ deg} \quad (6)$$

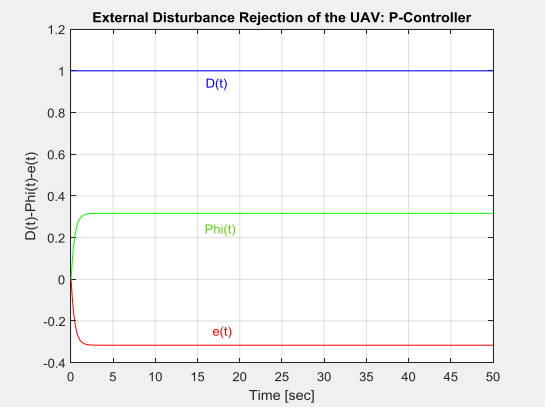

FIG. 6 Analysis of the Disturbance Rejection Ability of the UAV (MATLAB-script: R. Szabolcsi).

The error signal can be derived as:

$$e(\infty) = -\phi(\infty) \cong -0{,}3163 \text{ deg} \tag{7}$$

From equation (7) it is easy to discover that the UAV P-controller is unable to eliminate unwanted consequences of the external disturbance *D(t)*, and there is a remaining static error measured in zero value roll angle stabilization process.

If the disturbance *D(t)* represents the 0-Type, or 1-Type (single integrator) disturbance signal, unwanted effects from those mentioned above signals can be totally eliminated with no static error. If the disturbance *D(t)* behaves with 2-Type (double integrator) feature, there is a remaining static error measured for zero roll angle holding. Finally, if the closed control system is subjected to the 3-Type (triple integrator), or, higher type disturbances, the closed loop control system will diverge, losing its stability.

It is well-known from automatic control systems' theory that such case can be handled and static error can be eliminated using PI-controller instead of the static gain of K_c with the following model:

$$Y_c = K_c + \frac{1}{sT_I} = \frac{sT_I K_c + 1}{sT_I}; \quad K_c = 3{,}1623 \ {}^{V}/_{deg}; \quad T_I = \frac{1}{K_I} = 10 \text{ s} \tag{8}$$

Using PI-controller described in equation (8) reference signal tracking ability of the UAV closed loop control system has been tested. Results of the computer simulation can be seen in FIG. 7.

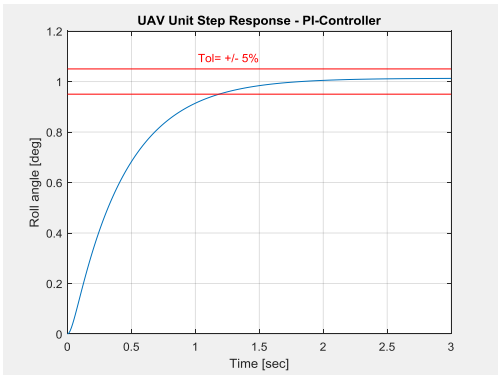

(a) $\phi_{ref}(t) = 1 * 1(t)\ deg$

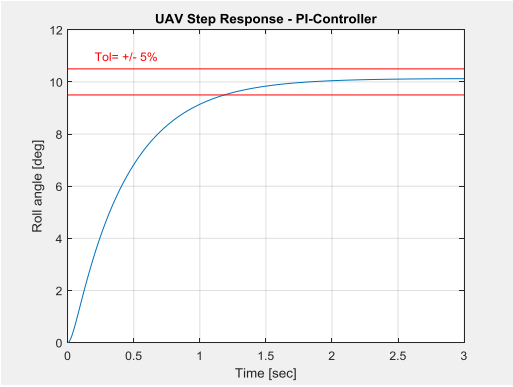

(b) $\phi_{ref}(t) = 10 * 1(t)\ deg$

FIG. 7 Time Domain Analysis of the UAV Closed Loop Automatic Flight Control System. (MATLAB-script: R. Szabolcsi).

From FIG. 7 it is easily can be seen that if to apply 5% of tolerance field to derive settling time, for the case when the UAV autopilot is subjected to a unit step change in roll angle, the settling time is ≈ 1,2 sec. For more agile and aggressive maneuvers, when the desired value of the roll angle at the closed loop control system input is 10 deg., the settling time is increased till that of ≈ 1,7 sec. That kind of the increase of the settling time related to that value of the case when UAV is controlled by P-controller, sometimes, can't be tolerated. The closed loop system time domain response can be accelerated via applying the D-term in the controller framework, or via applying the lead-compensator scheduled proper way.

Stability of the roll angle autopilot closed loop control system also can be evaluated using FIG. 8 [19, 20]. From FIG. 8 it is evident that calculated closed loop poles are negative ones, i.e. they lie on the left-hand side of the complex plain. This means, that closed loop system time domain behavior is stable, being aperiodic, exponential one, and settling time t_{ss} mostly determined by the pole located at *(-2,4+0*j)*. The system has a zero (FIG. 8) located at*(-0,0316+0*j)* cancelling the pole of the closed loop control system located at *(-0,0321+0*j)*.

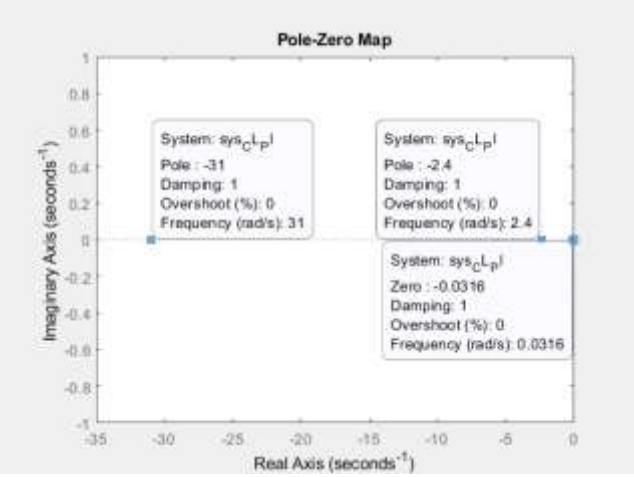

FIG. 8 Pole-Zero Map of the UAV Closed Loop Automatic Flight Control System – PI-Controller Case (MATLAB-script: R. Szabolcsi).

The closed loop control system stability based upon PI-controller is evaluated using open loop system Bode diagram, which can be seen in FIG. 9 [19, 20].

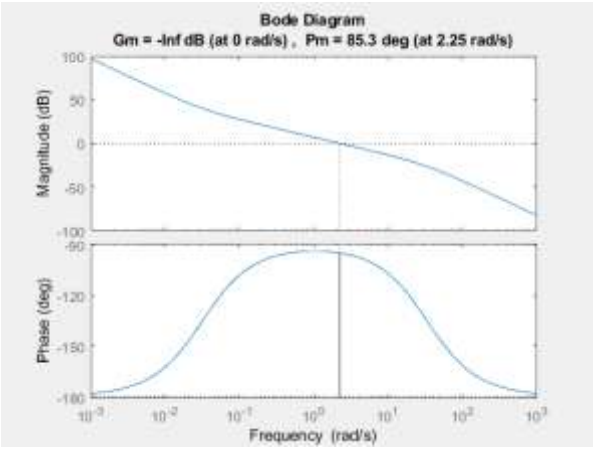

FIG. 9 UAV Open Loop System Bode Diagram PI-Controller Case (MATLAB-script: R. Szabolcsi).

Comparing Bode diagrams of the UAV closed loop control system based upon P-controller (FIG. 5), and the UAV closed loop control system based on PI-controller (see FIG. 9) it is evident, that phase margin is increased to that of 85,3 deg at crossover frequency of 2,25 rad/s, which stands for more robust closed loop control system. From FIG. 9 it is easy to see that the open loop control system based upon PI-controller is the 2-Type system due to open loop transfer function of the form:

$$Y_{O.L.} = \frac{(1+31{,}623s)}{10s}\,\frac{1}{(16.767+0{,}0502s)}\,\frac{1}{s} \tag{9}$$

The gain curve starts with slope of - 40 dB/D, After, at frequency of $^{1}/_{K_c T_I} = 0{,}0316\ 1/s$ derivative term in the numerator starts to introduce slope of +20 dB/D, and resulting slope of the gain curve streams to slope of - 20 dB/D. Finally, at frequency of $^{1}/_{0{,}0502}$ 1/s and after, the first order term will start to change slope of the gain curve for -20 dB/D. At the crossover frequency of 2,25 rad/s the slope of the gain curve is -20dB/D, i.e. the closed loop control system of the UAV is stable. However, the crossover frequency is changed from its initial value of 3,72 rad/s to that of 2,25 rad/s. The open loop control systems of the UAV can be compared using FIG. 10.

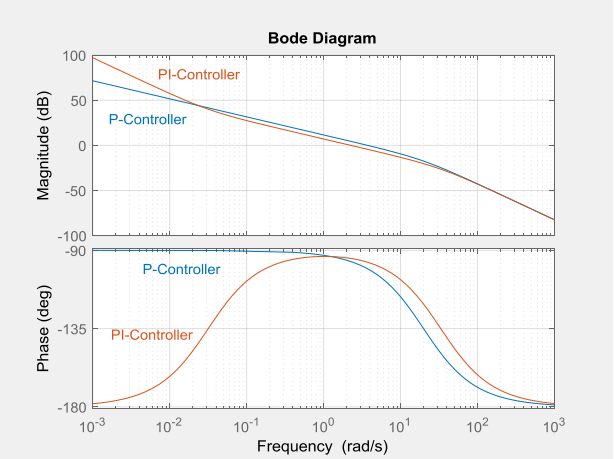

FIG. 10 UAV Open Loop System Bode Diagram: P-Controller vs PI-Controller Case (MATLAB-script: R. Szabolcsi).

From FIG. 10 It is evident that the crossover frequency ω_c is decreased. It is well-known from theory of automatic control systems that approximated settling time t_{ss} lies in between the range of:

$$\frac{\pi}{\omega_c} \leq t_{ss} \leq \frac{3\pi}{\omega_c} \tag{10}$$

From Eq. (10) it is easy to conclude that any decrease in crossover frequency ω_c will tend the UAV closed loop control system to increase its settling time t_{ss}.

FIG. 11 serves to compare time domain responses of those two controllers, being P-, or PI-type ones, implemented in the closed loop control system of the UAV in reference signal tracking missions.

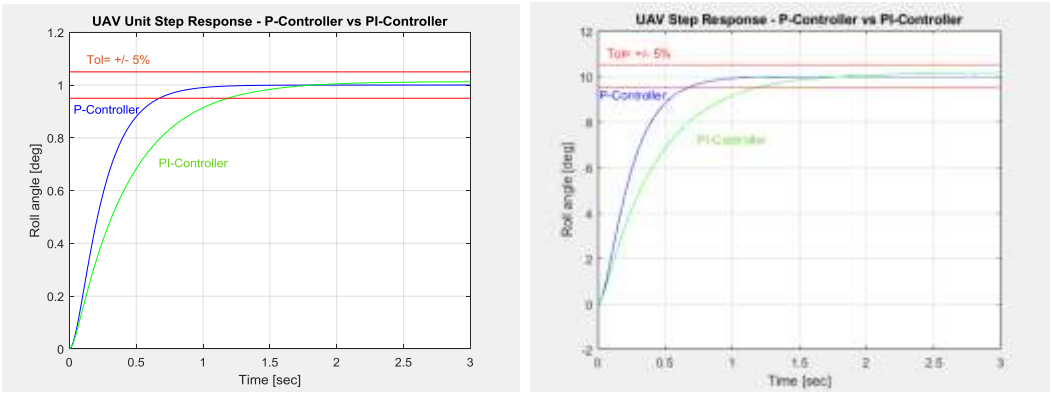

(a) $\phi_{ref}(t) = 1 * 1(t)\ deg$ (b) $\phi_{ref}(t) = 10 * 1(t)\ deg$

FIG. 11 Time Domain Analysis of the UAV Closed Loop Automatic Flight Control System. (MATLAB-script: R. Szabolcsi).

The advantage of the PI-Controller is in ability to omit unwanted effects generated by the external disturbance *D(t)*. The UAV closed loop control system depicted in FIG. 2 has been tested for disturbance rejection ability. Results of the computer simulation are highlighted in FIG. 12 [19, 20].

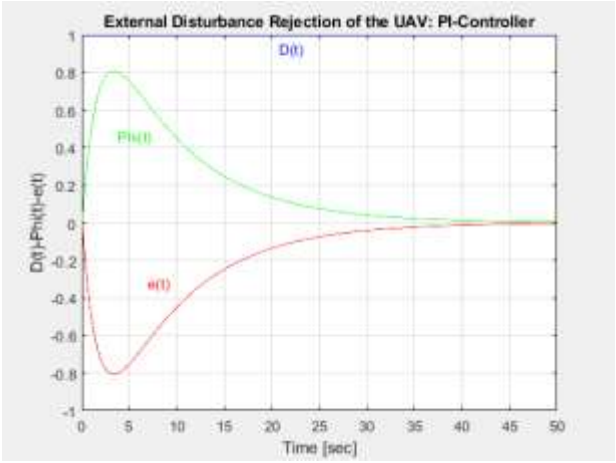

FIG. 12 Analysis of the Disturbance Rejection Ability of the UAV (MATLAB-script: R. Szabolcsi).

Regardless to emphasize that PI-controller is able to wash out (FIG. 12) unwanted effects from external disturbances, and, the zero roll angle reference can be kept to be constant, which is a case in many typical flight phases like cruising, circling, etc.

FIG. 13 serves to compare time domain responses of those two controllers being implemented in the closed loop control system of the UAV in analysis of the external disturbance rejection capabilities.

From FIG. 13. it is evident that PI-controller will perform well in disturbance rejection missions, however, settling time is increased to that value of $t_{ss} \cong 27\ sec$, what is a bottleneck of the application of the traditional PI-controller.

The early discussions of this paper stated that settling time can be increased via introducing D-term in the controller structure (FIG. 1.). As the first approximation, let us suppose that controller transfer function is as follows:

$$Y_c = K_c + \frac{1}{sT_I} + sT_D = \frac{sT_IK_c+1+s^2T_DT_I}{sT_I};\ \ K_D = T_D \tag{11}$$

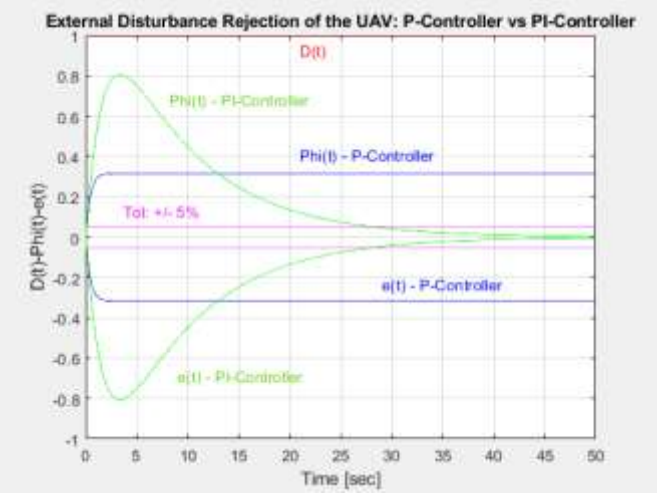

FIG. 13 Time Domain Analysis of the UAV Closed Loop Automatic Flight Control System. (MATLAB-script: R. Szabolcsi).

It is evident that equation (11) describes the *not proper* controller transfer function due to higher order '*s*' polynomial of the numerator than denominator has. To eliminate that bottleneck the order of the denominator '*s*' polynomial must be increased to that of two as per the minimum so as to get proper, or as the best strictly proper dynamic model of the controller. Thus, one might have such approximation of the lead controller transfer function:

$$Y_c = K_c + \frac{1}{sT_I} + sT_D \cong \frac{sT_IK_c+1+s^2T_DT_I}{sT_I(1+sK)}; \quad K \to 0 \tag{12}$$

It is worth to mention that PID-controller itself represents the band-rejection filter. The Bode diagram of the previously applied PI-controller and the augmented PID-controller is depicted in FIG.14.

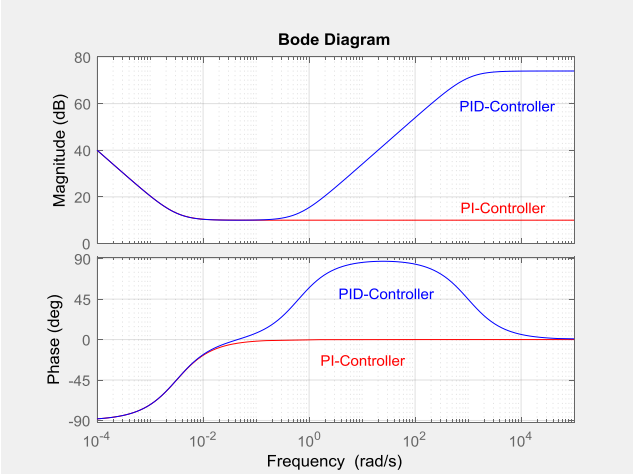

FIG. 14 Frequency Response Functions of the PI-, and augmented PID-Controllers. (MATLAB-script: R. Szabolcsi).

From FIG. 14. it can be easily seen that PI-controller represents the low-pass filter, whilst the PID-controller is the band-stop one, and further scheduling of the controller parameters like K_c, T_I, T_D, and finally, K, is necessary.

Second way to increase crossover frequency ω_c determining settling time t_{ss} (see Eq. 10) is to select the lead-compensator being active or passive, for control purpose. The transfer function of the lead compensator is as follows:

$$Y_{lead} = K_{lead}\frac{1+sT_1}{1+sT_2};\ \ 0 < \mathrm{K}_{lead};\ \ T_1 > T_2 \tag{13}$$

Using Fig. 10. the lead compensator parameters are chosen to be:

$$T_1 = 10\ sec;\ T_2 = 0{,}03\ sec;\ K_{lead} = 200 \tag{14}$$

The forward path enhanced PI-controller transfer function, leaning on Eq. (8) and Eq. (13), will have the form of:

$$Y_c = \frac{sT_IK_C+1}{sT_I}\mathrm{K}_{lead}\frac{T_1s+1}{T_2s+1} \tag{15}$$

The Bode diagram of the previously applied PI-controller and the PI controller enhanced with the lead compensator is represented in Fig. 15. From Fig. 15. it is evident that the proposed enhanced PI controller behaves like a band-stop filters do, and the proposed enhanced PI controller increases open loop gain sufficiently compared to that of the gain provided by the PI-controller.

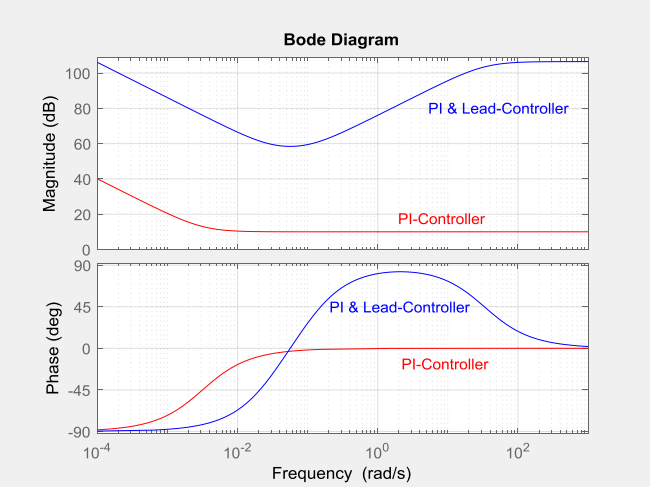

FIG. 15 Frequency Response Functions of the PI-, and enhanced PI-Controllers. (MATLAB-script: R. Szabolcsi).

Finally, comparison of those three controllers represented in this article, say, PI-, augmented PID-, and enhanced PI controllers can be conducted using FIG. 16 [19, 20].

Using FIG. 16. the frequency domain behavior of those three controllers mentioned above can be evaluated. The gain provided by the active enhanced PI-controllers increase gains sufficiently. The positive phase angle shift is tightened in the mid frequency range, compare to that of the PID-controller proposed.

The closed loop system of the UAV roll angle control system has been tested in time domain. Results of the computer simulation can be seen in FIG. 17.

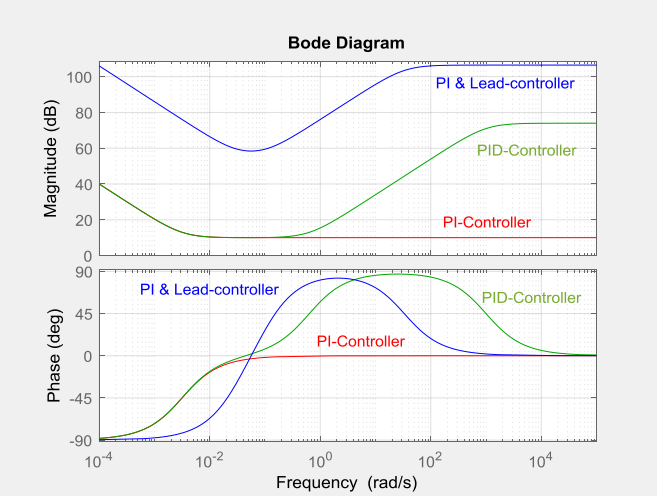

FIG. 16 Bode Diagrams of the PI-, augmented PID, and enhanced PI-controllers. (MATLAB-script: R. Szabolcsi).

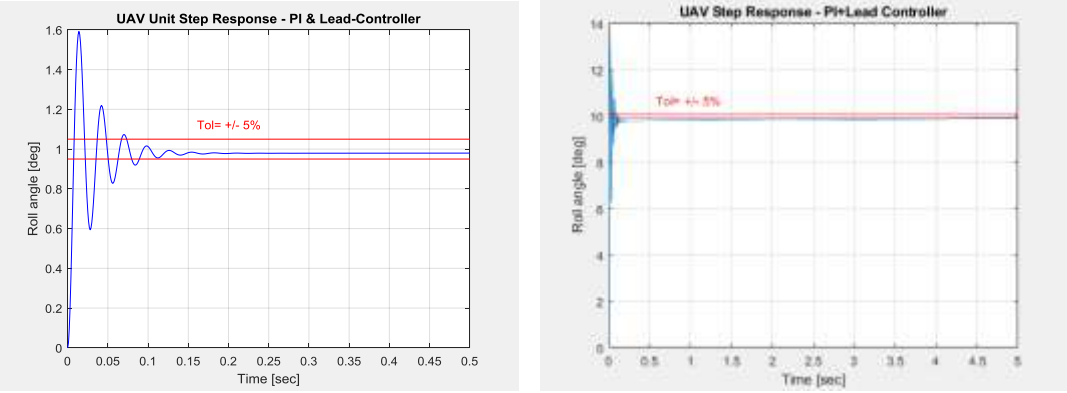

(a) $\phi_{ref}(t) = 1 * 1(t)\ deg$ (b) $\phi_{ref}(t) = 10 * 1(t)\ deg$

FIG. 17 Time Domain Analysis of the UAV Closed Loop Automatic Flight Control System. (MATLAB-script: R. Szabolcsi).

Using FIG.17 it is evident that the UAV roll angle closed loop control system has significantly faster response to its roll angle references. For the unit step input the settling time is decreased to that of 0,1 sec. The only disadvantage is that the roll angle closed loop control system became more oscillatory. If the percent overshoot is out of the range being defined in advance, further schedule of the forward controller parameters in needed.

Time domain behavior of those systems having PI-, and enhanced PI controllers can be compared using FIG. 18.

Using FIG. 18 It can be stated that both transient peak time and settling time were improved if to implement enhanced PI controller, which eliminates bottleneck of the traditional PI controller's increasing settling time of the closed loop roll angle control system of the UAV.

The UAV roll angle open loop control system based upon enhanced PI controller Bode diagram can be seen in FIG. 19, and, comparison of the three controllers proposed for use in this paper can evaluated using FIG. 20 [19, 20].

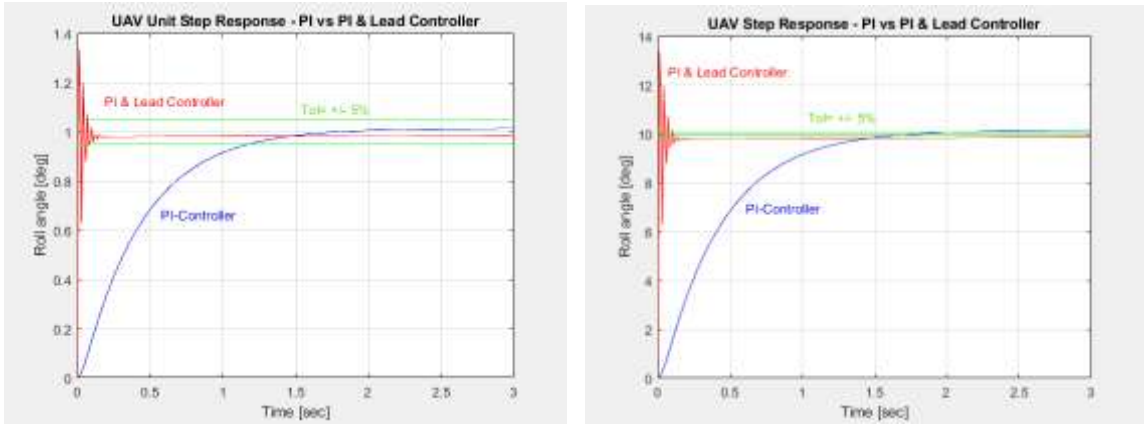

(a) $\phi_{ref}(t) = 1 * 1(t)\ deg$ (b) $\phi_{ref}(t) = 10 * 1(t)\ deg$

FIG. 18 Time Domain Analysis of the UAV Closed Loop Automatic Flight Control System. (MATLAB-script: R. Szabolcsi).

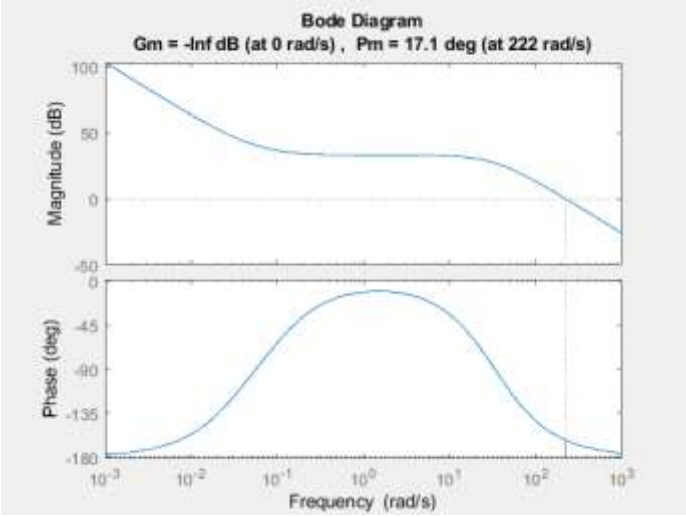

FIG. 19 UAV Open Loop System Bode Diagram: enhanced PI Controller Case (MATLAB-script: R. Szabolcsi).

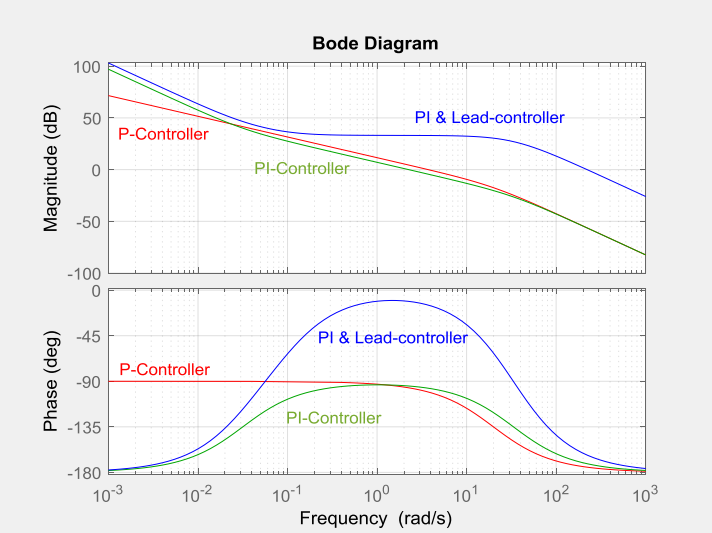

FIG. 20 Bode Diagrams of the Open Loop Control Systems of the UAV. (MATLAB-script: R. Szabolcsi).

From FIG. 19 it is evident that crossover frequency in increased from that value of 2,25 rad/s (PI controller case) to its new value of 222 rad/s, i.e. settling time defined by Eq (10) is decreased, and, the UAV roll angle closed loop control system became more faster.

The only feature remained to be examined is the time domain analysis of the UAV roll angle closed loop control system in disturbance rejection mission. In that fashion, the external disturbance *D(t)* is supposed to behavior with unit step function.

Leaning on final value theorem of the Laplace transformation yields to:

$$\lim_{t\to\infty}\phi(t)=\lim_{s\to 0}s\phi(s)=\lim_{s\to 0}sW_D\,(\mathrm{s})\mathrm{D}(\mathrm{s})=\lim_{s\to 0}W_D\,(\mathrm{s})=\frac{0{,}3588s^2+11{,}96s}{0{,}01506s^4+1{,}0051s^3+73944{,}33s^2+9730{,}756s+233{,}8}=0\ \mathrm{deg} \tag{16}$$

The UAV roll angle closed loop control system was tested for disturbance rejection ability. Results of the computer simulation can be seen in FIG. 21.

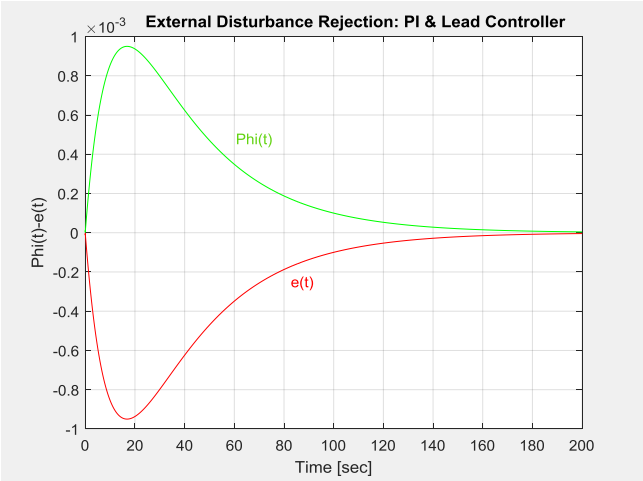

FIG. 21 Time Domain Analysis of the UAV Closed Loop Automatic Flight Control System. (MATLAB-script: R. Szabolcsi).

From FIG. 21 it is evident that the UAV roll angle closed loop control system based upon enhanced PI controller is able to eliminate consequence of the external disturbance, which is a Type-1 input signal. It is well-known that the proposed enhanced PI controller would not degrade the open loop system type, which is equal to that of 2. In other words, the disturbance rejection ability of the newly proposed enhanced PI controller will ensure the ideal disturbance rejection, and, additionally, will accelerate the UAV roll angle closed loop control system responses. Regarding Eq (14) the enhanced PI controller is an active one, and its gain is 200, which is the only disadvantage of the proposed controller. However, the gain needed to build up the controller will not generate any difficulties in control engineering of recent days.

4. CONCLUSIONS

The behind this research work was to solve the selection of the optimal controllers, and tune controllers for the new frameworks improving disturbance rejection ability of the UAV roll angle closed loop control systems.

Leaning on static controllers of the previously solved LQR design problem, few of the available controllers like traditional PI controllers, or PID controllers had been analyzed.

The PI controller is a framework able to eliminate unwanted effects from external disturbances. However, the integral feature will decrease open loop system crossover frequency, which tends the closed loop control system for slower responses.

To eliminate this disadvantage the PID controller and the enhanced PI controller were introduced. Analytical studies and computer simulations both in time and in frequency domains had shown that the proposed enhanced PI controller will keep property of the closed loop system leaning on PI controller to eliminate unwanted effects from external disturbances, whilst to eliminate disadvantage of the PI controller decelerating the closed loop control system. Moreover, the proposed enhanced PI controller accelerated the closed loop control system of the UAV via increasing its crossover frequency.

REFERENCES

[1] Békési Bertold, Szegedi Péter: *Preliminary Design of Controller of Longitudinal Motion of the Unmanned Aerial Vehicle Using LQR Design Method*. Proceedings of the 10th International Conference: Transport Means 2006, Kaunas, Lithuania, pp. 324-327.

[2] Eng, P. C. S. *Path Planning, Guidance and Control for a UAV Forced Landing.* PhD Thesis, Queensland University of Technology, Australia, 2011.

[3] Békési Bertold, Wührl Tibor: *Redundancy for micro UAVs – control and energy system redundancy*. Proc. of the International Conference Deterioration, Dependability, Diagnostics 2012, Brno, Czech Republic, pp. 123-130. (ISBN:978-80-7231-886-5).

[4] Batmaz, A. U., Elbir, O., Kasnakoglu, C. (2013): Design of a Quadrotor Roll Controller Using System Identification to Improve Empirical Results. *International Journal of Mechanics and Manufacturing*. Vol 1, No4, pp(347-349), 2013.

[5] Bolandi, H., Rezaei, M., Mohnesipour, R., Nemati, H., Smailzadeh, S. M. (2013): Attitude Control of a Quadrotor with Optimized PID Controller. *Intelligent Control and Automation*. Vol 4, pp(335-342), 2013.

[6] Jose, C.V., De Paula, J.C., Leandro, G.V., Bonfim, M.C. (2013): Stability and Control of a Quad-Rotor Using a PID Controller. *Brazilian Journal of Instrumentation and Control*. Vol 1, No1, pp(15-20), 2013.

[7] Haq, A. U., Reddy, S. G.M., Raj, C. P. P. (2014): Design, modeling and Tuning of Modified PID Controller for Autopilot in MAVs. *International Journal of Sciences & Engineering Research*. Vol 5, Issue 12, pp(506-513), 2014.

[8] Koszewnik, A. (2014): The Parrot UAV Controlled by PID Controllers. *Acta Mechanica et Automatica*. Vol 8, No2, pp(65-69), 2014.

[9] Tanveer, M.H., Hazry, D., Ahmed, S. F., Joyo, M.K., Warsi, F. A., Razlan, Z.M., Wan, K., Hussain, A.T. (2014): PID Based Controller Design for Attitude Stabilization of Quad-rotor. *Australian Journal of Basic and Applied Sciences*. Vol 8(4), pp(1-5), 2014.

[10] V. Șandru, M. Rădulescu: The Use of UAV's During Actions of Integrated Air Defense Systems. *Review of the Air Force Academy*, No 3 (30) 2015, pp (133-138), 2015.

[11] Alaimo, A., Artale, V., Barbaraci, G., Milazzo, C.L.R., Orlando, C., Ricciardello, A. (2016): LQR-PID Control Applied to Hexacopter Flight. *Journal of Numerical Analysis, Industrial and Applied Mathematics*. Vol 9-10, No3-4, pp(47-57), 2016.

[12] Praveen, V., Pillai, A. S. (2016): *Modeling and Simulation of Quadrotor Using PID Controller*. *IJCTA*. 9(15), pp(7154-7158), 2016.

[13] Szabolcsi, R. (2016). *Automatic Flight Control of the UAV.* Budapest: Óbuda University.

[14] S. Pop, A. Luchian, R. G. Zmădu, E. Olea: The Evolution of Unmanned Aerial Vehicles. *Review of the Air Force Academy*, No.3 (35)/2017, pp(125-132), 2017.

[15] Sattar, M., Ismail, A. (2017): PID Control of a Quadrotor UAV. *International research Journal of Engineering and Technology.* Vol 04, Issue 8, pp(1490-1493), 2017.

[16] Satla, Z., Elajrami, M., Bendine, K. (2018): Easy Tracking of UAV Using PID Controller. *Periodica Polytechnica Transportation Engineering*. (Accessed 3 July 2018 at https://pp.bme.hu/tr/article/view/10838).

[17] Sendoya-Losada, D.F., Quinterro-Polanco, J.D.(2018): PID Controller Applied to an Unmanned Aerial Vehicle. *ARPN Journal of Engineering and Applied Sciences.* Vol 13, No1, pp(325-334), 2018.

[18] Szabolcsi, R.: Design and Development of the LQR Optimal Controller for the Unmanned Aerial Vehicle. *Review of the Air Force Academy No.1 (36)/2018., pp(45-54.)*

[19] MATLAB 9.4 (R2018a), User's Guide, The MathWorks, 2018.
[20] MATLAB 9.4 Control System Designer/Control System Toolbox 10.4, User's Guide, The MathWorks, 2018.
[21] *www.micropilot.com* (Accessed 11 September 2018).
[22] *http://paparazzi.enac.fr (*Accessed 11 September 2018).